Associations Between the Principal Spatial Modes of North American Prairie Snow Water Equivalent and Low-Frequency Atmospheric Circulation

C. DERKSEN,[1] E. LEDREW,[2] A. WALKER,[2] AND B. GOODISON[2]

ABSTRACT

Ten winter seasons (December, January, February 1988/89 to 1997/98) of passive microwave derived snow water equivalent (SWE) imagery are utilized to examine the seasonal snow cover characteristics of a ground-validated North American Prairie study area. The images are derived from Special Sensor Microwave/Imager (SSM/I) brightness temperatures, processed with the Canadian Atmospheric Environment Service dual channel SWE retrieval algorithm. The ten-season time series of five day averaged (pentad) imagery was subjected to a rotated principal components analysis in order to isolate the dominant spatial modes of SWE within the study period. The component loading patterns were then cross correlated (with time lags) to monthly averaged atmospheric teleconnection indices (East Pacific - EP, Pacific/North America - PNA, and North Atlantic Oscillation - NAO patterns). Results indicate that the monthly indices are weakly associated, in any systematic manner, to the dominant spatial modes of Prairie snow cover, although linkages can be identified with a case by case approach. Analysis of pentad resolution atmospheric data yields stronger results because the transient nature of winter Prairie snow cover is better captured by these data. Both Prairie SWE and SCA anomalies are shown to be poorly autocorrelated through time, further illustrating the need for synoptically sensitive data.

Key words: passive microwave, snow water equivalent, atmospheric teleconnections, time lagged correlation.

INTRODUCTION

The forcing relationships between snow cover and atmospheric circulation are difficult to isolate because of the complex nature of their interaction. Single cyclonic events can extend or reduce regional snow extent dramatically, while the presence or absence of snow cover modifies energy exchange between the surface and atmosphere. Empirical signals between snow cover and atmospheric circulation are thereby complicated by the ambiguity inherent to the inter-relationships between snow cover, temperature, and circulation (Cohen and Rind, 1991). Conversely, specific atmospheric patterns favour precipitation in certain regions, thereby allowing snow cover distribution to be a consequence of specific atmospheric configurations (Walsh, 1984).

In this study we seek to address the conflict between these perspectives by relating North American Prairie snow cover to archived atmospheric teleconnection indices (North Atlantic Oscillation - NAO, Pacific/North America - PNA, and East Pacific - EP). Eigenanalysis of long time series of gridded atmospheric data has confirmed the existence of numerous teleconnection

[1] Waterloo Laboratory for Earth Observations, Department of Geography, University of Waterloo, Waterloo, Ontario N2L 3G1, Canada

[2] Climate Research Branch, Atmospheric Environment Service, 4905 Dufferin Street, Downsview, Ontario N3H 5T4, Canada

patterns (Wallace and Gutzler, 1981; Lanzante, 1984; Barnston and Livezy, 1987), which are of interest because they capture preferred low-frequency configurations of atmospheric standing wave structures. These patterns consistently appear on a seasonal and annual basis, creating inherent predictive potential. Another appeal is their simplicity: a single standardized value indicates the phase and magnitude of a given pattern.

Previous studies have related teleconnection patterns to terrestrial snow cover at various spatial and temporal scales. The positive phase of the PNA, expressed through strong ridging over western North America, has been associated with deficit snow cover in the North American Prairies and American Rockies (Gutzler and Rosen, 1992; Cayan, 1996). Associations between the PNA, EP, and Tropical/Northern Hemisphere (TNH) patterns have been isolated for the eastern United States (Serreze et al., 1998), while Clarke et al. (1999) have linked three preferential teleconnections with Eurasian snow cover. These studies have correlated atmospheric patterns to snow cover distribution and subsequently identified teleconnections embedded in the circulation patterns. In this study, we take a different approach by examining correlations (with time lags) between snow cover diagnostics and archived teleconnection indices furnished by the National Oceanic and Atmospheric Administration (NOAA). The general objective is to investigate the predictive potential of linking index phase and magnitude to central North American snow distribution.

Utilizing a ten season (December, January, February 1988/89 -1997/98) time series of five day averaged (pentad) passive microwave derived snow water equivalent (SWE) imagery, the specific objectives of this study are:

1. Using a rotated principal components analysis (PCA) of pentad resolution imagery, identify the dominant spatial modes of Prairie SWE and the associated temporal persistence of these modes. Are trends in snow accumulation modes evident through the time series? How do component patterns and persistence relate to Prairie SWE and snow covered area (SCA) anomalies calculated for the time series?
2. Explore time lagged correlations between component loading patterns, standardized SWE and SCA anomalies, and teleconnection indices at a monthly temporal resolution. Are there systematic associations between SWE distribution, snow extent, and atmospheric teleconnections? Can the phase and magnitude of teleconnection patterns be used to predict a response in snow distribution? How does the temporal degradation of pentad SWE data to monthly averages influence correlation results?

DATA

Rapid scene revisit capabilities, all-weather imaging, and the ability to derive quantitative estimates of SWE make passive microwave imagery suitable for monitoring terrestrial snow cover (Grody and Basist, 1996; Foster et al., 1997; Tait, 1998). The ability to distinguish snow covered and snow free land in the microwave portion of the electromagnetic spectrum is a function of changes in microwave scatter caused by the presence of snow crystals. For a snow covered surface, microwave brightness temperature decreases with increasing snow depth because the greater number of snow crystals provides increased scattering of the microwave signal. This simple relationship, however, is complicated by a range of physical parameters (Table 1) which place spatial and temporal limitations on the use of passive microwave imagery for monitoring snow cover.

The Canadian Atmospheric Environment Service (AES) has developed and evaluated single and dual frequency passive microwave algorithms for determining SWE in the North American Prairies through an intensive satellite/airborne/ground experiment in central Canada (Goodison et al., 1986). An overview of the algorithms, and their strengths and weaknesses, is provided by Goodison and Walker (1994). The AES dual frequency algorithm used in this study utilizes the brightness temperature gradient between 19 and 37 GHz Special Sensor Microwave/Imagery (SSM/I) channels in the EASE-Grid (Equal Area SSM/I Earth) projection. Grid spacing is 25 km for the 19 and 37 GHz frequencies, although the actual SSM/I footprint size is 60 and 30 km respectively for these channels. The data were obtained from the National Snow and Ice Data Center in Boulder, Colorado. After processing the brightness temperatures with the dual channel AES algorithm, a 70 by 40 pixel Prairie subscene was identified for further analysis (Figure 1).

Table 1. Parameters influencing interaction between microwave energy and the snowpack.

Parameter	Influence on Microwave Energy
Snow Wetness	Wet snow approaches black body behaviour; between channel brightness temperature gradient degrades; snow cover becomes "invisible".
Ice Crusts	Alters absorption and emission characteristics; Increases emissivity at high frequencies relative to low frequencies.
Depth Hoar and Crystal Structure	Large crystals increase snowpack scatter, artificially increasing retrieved SWE.
Snow Depth	At a maximum of approximately 1 metre depth, relationship between brightness temperature and SWE weakens.
Temperature	Large temperature gradients contribute to depth hoar formation; temperature physically associated with snow wetness.
Soil Conditions	Soil type and wetness can influence emissivity.
Vegetative Cover	Wide ranging effects: contributes scatter, absorption, and emission.

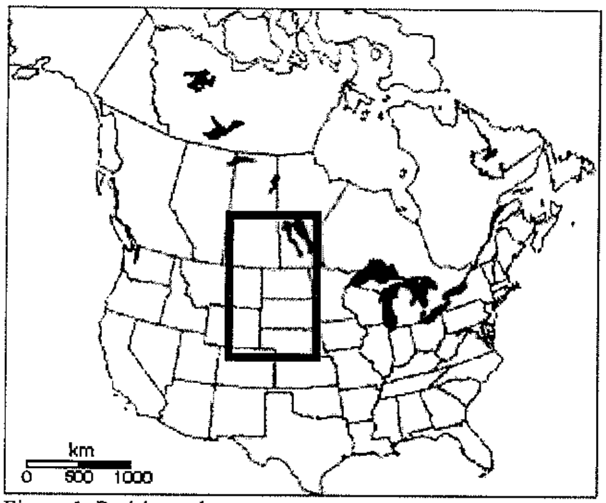

Figure 1. Prairie study area.

The dual frequency algorithm performs strongly when snowpack conditions are deep and dry, achieving 10 to 20 mm agreement with surface sampling (Goodison and Walker, 1994). Problems occur when fresh snow is deposited on a warm surface, and when attempting to discriminate between melting snow areas and snow free land (Walker and Goodison, 1993). For these reasons, winter months were selected for analysis, and data from morning overpass times were used to mitigate the influence of melt. These two decisions have proven to effectively limit regional underestimation of snow cover by passive microwave imagery (Derksen and LeDrew, 1999). The SWE imagery span 10 winter seasons (DJF 1988/89 - 1997/98) at a temporal resolution of five days. 18 pentads extend from December 2 to February 29/March 1 as outlined in Table 2. Table 3 summarizes the missing pentads from the time series, which can be attributed to incomplete Prairie coverage within a pentad period primarily caused by data storage and transfer problems on the orbiting platform.

Table 2. Summary of pentad structure.

Pentad	Time Span	Pentad	Time Span
68	Dec. 2 to Dec. 6	04	Jan. 16 to Jan. 20
69	Dec. 7 to Dec. 11	05	Jan. 21 to Jan. 25
70	Dec. 12 to Dec. 16	06	Jan. 26 to Jan. 30
71	Dec. 17 to Dec. 21	07	Jan. 31 to Feb. 4
72	Dec. 22 to Dec. 26	08	Feb. 5 to Feb. 9
73	Dec. 27 to Dec. 31	09	Feb. 10 to Feb. 14
01	Jan. 1 to Jan. 5	10	Feb. 15 to Feb. 19
02	Jan. 6 to Jan. 10	11	Feb. 20 to Feb. 24
03	Jan. 11 to Jan. 15	12	Feb. 25 to Feb. 29/March 1

Table 3. Pentads omitted from PCA due to incomplete Prairie coverage.

Season	Omitted Pentads
1988/89	8903
1989/90	None
1990/91	9072
1991/92	9172, 9173
1992/93	9306, 9312
1993/94	9407-9412
1994/95	None

Total Prairie snow covered area (SCA) was derived for each pentad of SWE imagery by summing the total number of snow covered pixels (SWE > 0) and multiplying by the EASE-Grid pixel resolution (25 km by 25 km). Standardized total Prairie SWE and SCA anomalies were also computed for each pentad based on the ten season mean and standard deviation.

Monthly atmospheric teleconnection indices for three patterns (NAO, EP, PNA) were acquired from NOAA. These data, along with documentation, are available online (nic.fb4.noaa.gov/data/cddb). The teleconnection patterns are computed from monthly mean 700 mb geopotential height anomalies which are subjected to a rotated PCA. The ten leading patterns for each calendar month are retained, and an amplitude is calculated for each using least-squares regression analysis. The amplitudes are then assembled into a continuous time series and standardized. If a teleconnection is not one of the ten leading modes, no amplitude is derived.

METHODS

Principal components analysis (PCA) was used to identify the dominant spatial modes of SWE within the ten-season time series of passive microwave derived imagery. PCA mathematically transforms a dataset into a reduced set of uncorrelated variables which represent the majority of the information contained within the original data. The use of principal components simplifies analysis of time series data by representing the entire dataset in a smaller number of images which proportionally explain the variance within the original data.

The SWE data were orthogonally transformed using the varimax rotation method which maximizes the sum of the variances of the squared loadings within each column of the loadings matrix (Richman, 1986). The PCA input matrix was composed of columns for each time series pentad, while SSM/I pixels comprised the rows. Not all pentads are represented in the time series because of incomplete study scene coverage (see Table 3); so the input matrix had 168 columns (pentads), and 2800 rows (pixels). Units of observation for the input data were millimetres. PCA was performed using a correlation matrix approach as opposed to a covariance matrix. Discussion has shown this method to be advantageous in synoptic climatological applications (Overland and Preisendorfer, 1982). The first seven components were subjectively retained for further investigation as one of these components provides the strongest loading for all pentads.

Principal components do not depict actual observable data patterns, but rather variance exhibited within the original data. In order to visualize the data that components are representing, the pentad of time series data that loads most strongly to each specific component are used in subsequent descriptions and figures. Through this procedure, the component loading patterns are utilized to identify real spatial patterns. The standardized total Prairie SWE and SCA anomalies calculated for each pentad are used to assist in the interpretation of PCA results, and to provide additional variables for correlation analysis.

Cross correlation analysis provides a means to link the dominant spatial patterns of snow cover as identified by the PCA, and atmospheric teleconnections as summarized by the monthly standardized indices. It also allows the addition of a temporal dimension to the analysis through time lagged correlation. In this study, cross correlation analysis was performed between the rotated SWE principal component loadings, the SWE and SCA anomaly series, and the NAO, EP, and PNA teleconnection indices. All variables were standardized. For this analysis, all pentad averaged information (loadings and anomalies) were degraded to monthly averages to allow correlation of temporally consistent data. Time lags of plus and minus one month were examined to investigate the degree to which the atmosphere leads snow cover and vice versa. While this statistical analysis cannot provide proof of cause and effect relationships, they can give insight into associations that may be validated by subsequent process studies. Lagged correlations have, for example, been utilized to investigate the direction of forcing between sea ice and the atmosphere (Walsh and Johnson, 1979).

RESULTS

A summary of the 10-season PCA is provided in Table 4. Seven components combine to explain the majority of the variance in SWE distribution through the time series. Subsequent components are not examined further as in no point in the time series do they have a higher loading than one of the first 7 components. The component loading pattern (Figure 2) illustrates the high degree of interannual variability in Prairie SWE. Only PC1 exhibits temporal persistence which extends to consecutive, multiple seasons. The remaining components serve to characterize individual seasons only, except for PC2 which loads strongly for 1993/94 and 1996/97.

Table 4. Summary of 10-season PCA results.

Component	Variance Explained (%)	Strongest Loading Pentad
PC1	25.2	9007
PC2	16.0	9702
PC3	15.0	9572
PC4	8.2	9272
PC5	7.6	9473
PC6	7.1	9802
PC7	3.8	8871
Remainder	17.1	

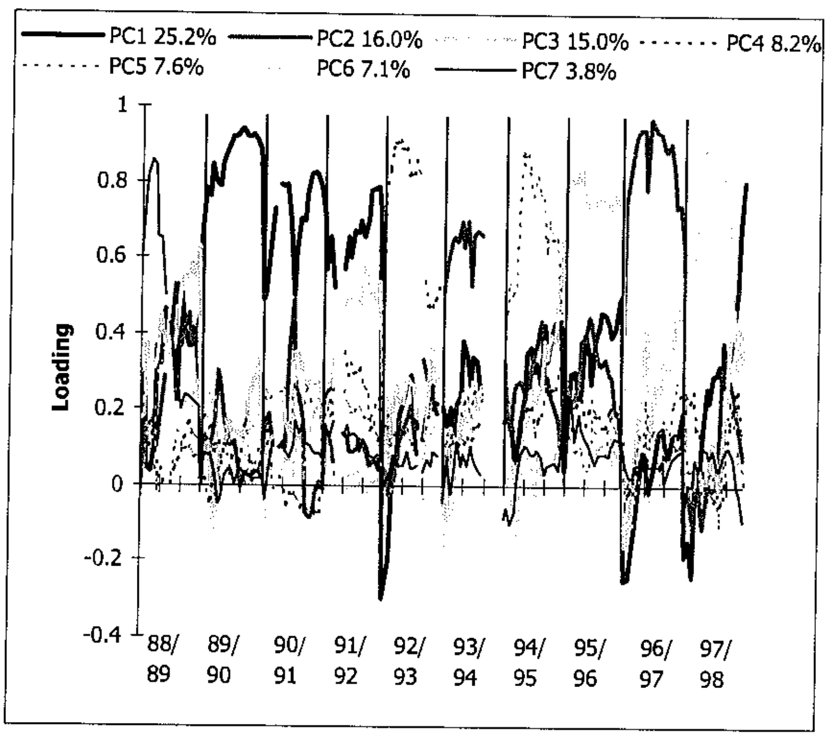

Figure 2. Component loading pattern for the 10-season PCA.

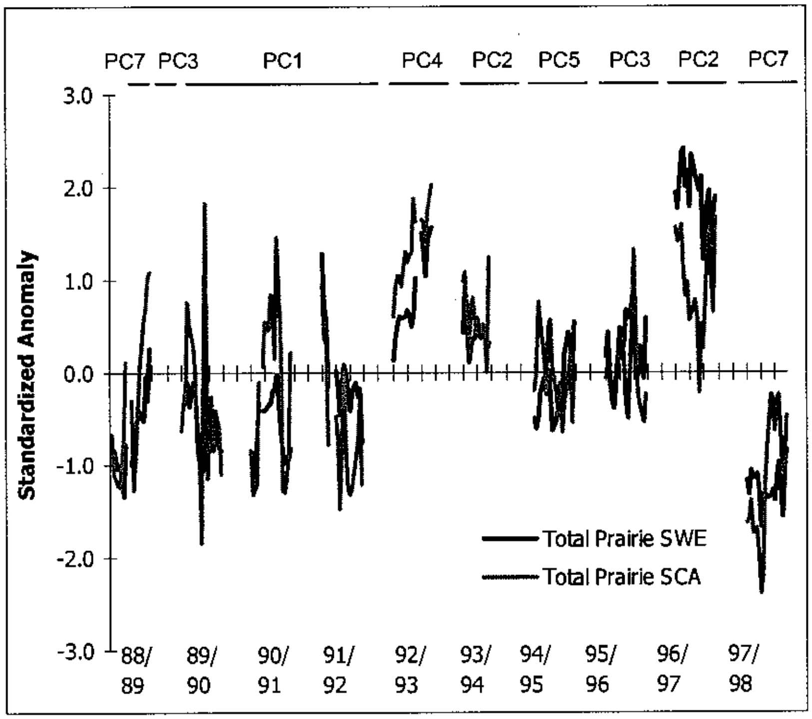

Figure 3. Association between standardized SWE and SCA anomalies, and dominant principal components.

The time series of standardized total Prairie SWE and SCA anomalies are shown in Figure 3. The constant evolution between "light" and "heavy" snow years is illustrated, with multiple components needed to capture these changes. It is also evident that similar anomalies can vary spatially. 1992/93 and 1996/97 are both heavy snow seasons, but are characterized by unique principal components. Likewise, 1988/89 and 1997/98 are light snow years, but also differ spatially. Although the SWE and SCA anomalies during 1994/95 and 1995/96 fluctuate around zero, two components are again significant for these two seasons. Other interesting features in the anomaly time series can be noted. First, there is no clear trend in passive microwave derived Prairie SWE or SCA. Anomalously positive and negative snow cover seasons are interspersed through the time series. Second, it is common to have coincident SWE and SCA anomalies of opposed signs. These periods can persist for multiple pentads, as in December, 1990. Third, rapid changes in anomaly phase and magnitude can be observed, indicating abrupt changes in snow extent and SWE due to both wide scale ablation and accumulation.

Spatially, the pentads which load most strongly to each component (Figure 4), also exhibit the variability in SWE extent and magnitude which is typical for the Prairie region. SWE extent varies from continuous and expansive (PC2) to discontinuous and sparse (PC6 and PC7). The regions of heaviest SWE concentration are also inconsistent, varying between the north (PC1), central (PC2, PC3, PC4), and southeast (PC5) of the study region.

Given the nature of North American Prairie SWE distribution as isolated by the PCA performed on pentad resolution imagery, it follows that a variety of atmospheric configurations would be associated with the variability in surface conditions. At a monthly temporal resolution, however, systematic correlations between the component loadings, SWE and SCA anomalies, and atmospheric teleconnection indices are generally weak (Figure 5). Some individual associations are relatively strong, such as the EP pattern leading PC7 by 1 month ($r=0.65$), but the overall correlations are not encouraging. Of note are the especially poor correlations when snow cover is treated as the leading variable: no correlations are stronger than $\pm$ 0.4.

While the monthly correlations are not convincing, a case by case approach does yield evidence of some relationships. The PNA index is generally of opposite sign to snow anomalies: 67% of occurrences for SWE, and 60% for SCA. In addition, for all cases where the EP pattern is positive,

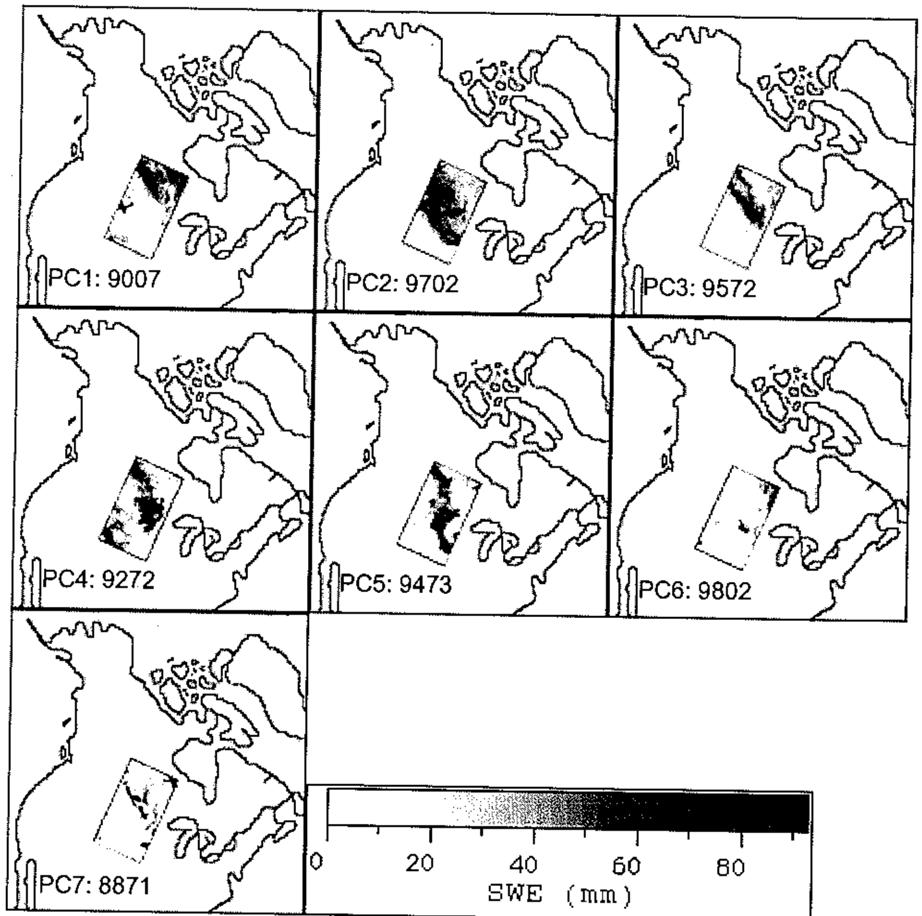

Figure 4. SWE imagery with the strongest loading to the first seven components.

both SWE and SCA anomalies are negative. These findings are confirmed by the correlation results. With both the atmosphere leading and no time lag, there is a negative correlation between both the EP and PNA patterns and SWE and SCA anomalies. These teleconnections are therefore associated with snow anomalies of the opposite sign with the atmosphere leading by one month. Any associations between the NAO and snow cover are not apparent at this temporal and spatial scale.

Since the correlation relationships between these monthly averaged diagnostics are generally weak, it is apparent that teleconnection indices are not appropriate as a sole predictor for Prairie snow cover conditions. However, the correlation results are not surprising given the level of association between snow cover and other climatological variables isolated by studies utilizing monthly averaged data. For instance, Walsh et al. (1982) found that only 5 to 20% of the variance in winter season United States temperature can be explained by snow cover. Foster et al. (1983) showed that only between 12 and 46% of North American winter temperatures can be explained by autumn and winter snow extent. Stronger regional results have been achieved linking snow cover to temperature departures (Karl et al., 1993; Leathers and Robinson, 1993), but coarse temporal resolution relationships between snow cover and climatological variables such as temperature stand to be improved by the integration of teleconnection indices. Finally, it is important to provide explanations for the poor monthly averaged correlation results from this, and other studies. Some potential causes are outlined below.

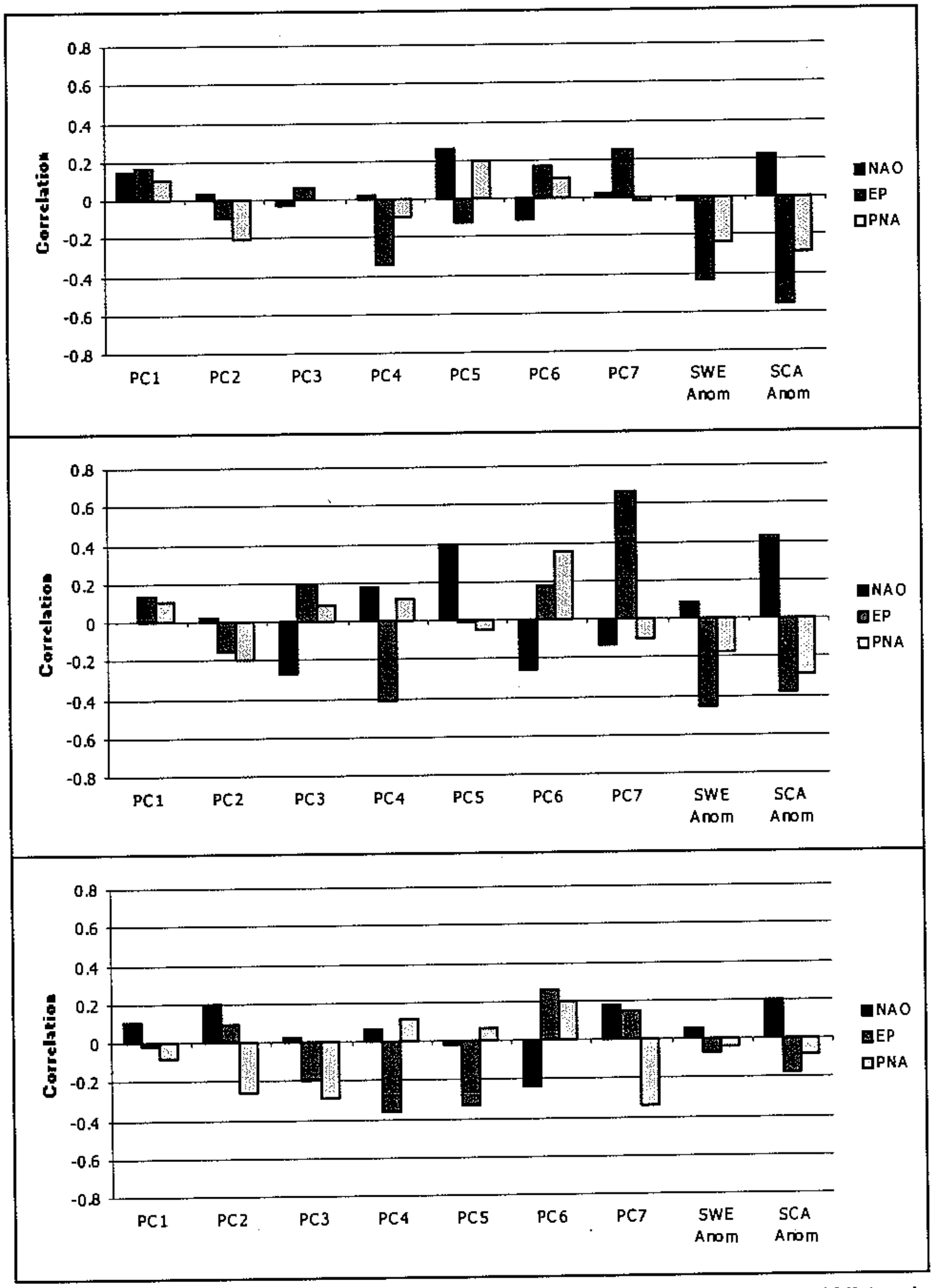

Figure 5. Cross correlation results with no time lag (top) the atmosphere leading (middle) and snow cover leading (bottom).

Snow Cover Anomaly Autocorrelation

Given the nature of both SWE and SCA anomalies for the North American Prairies (as shown in Figure 3), it is not surprising that rigorous systematic correlations were not discovered when using monthly averaged, temporally coarse data. First, the anomalies exhibit poor temporal persistence over time. Lagged autocorrelations for the SWE and SCA anomalies were calculated for each season (Table 5). For the majority of seasons (SWE: 7/10; SCA: 8/10) maximum autocorrelation exists at a lag of 1 pentad, showing that anomalies of similar phase and magnitude are generally of a duration ranging from only 5 to 10 days. Those seasons that have a longer lagged maximum autocorrelation typically have a correlation of low magnitude so they cannot be interpreted as significant, persistent anomaly structures.

Table 5. Temporal autocorrelation of total Prairie SWE anomalies.

Season	Lag of Maximum SWE Autocorrelation	Maximum SWE Autocorrelation	Lag of Maximum SCA Autocorrelation	Maximum SWE Autocorrelation
1988/89	2	0.56	1	0.74
1989/90	1	0.60	4	0.16
1990/91	1	0.73	1	0.62
1991/92	1	0.46	1	0.37
1992/93	1	0.72	1	0.59
1993/94	1	0.24	1	0.20
1994/95	1	0.57	1	0.37
1995/96	1	0.44	3	0.54
1996/97	3	0.28	1	0.41
1997/98	3	0.27	1	0.77

If a given anomaly is modified every 1 to 2 pentads, then a monthly summary anomaly is actually a composite of numerous unique anomalies, thereby failing to capture any physically relevant information. The anomaly autocorrelations show that the transient nature of central North American snow cover necessitates the use of synoptically sensitive data to isolate forcing relationships with the atmosphere. When other factors are considered, such as the existence of coincident SWE and SCA anomalies of opposite sign, this information underscores the complex relationship between snow cover and the atmosphere.

Synoptic Sensitivity

As previously suggested, anomaly autocorrelation results show that synoptically sensitive data are more appropriate for associations between snow cover and the atmosphere due to the transient nature of surface conditions. Although correlation of monthly teleconnection indices to monthly diagnostics of snow cover led to few decisive linkages in this study, the EP and PNA patterns were identified as being negatively associated with the anomaly phase of Prairie snow cover. Of interest, therefore, is the extent to which these low-frequency patterns are expressed within synoptically sensitive atmospheric fields.

Preliminary synoptic scale analysis of gridded atmospheric data is presented in Derksen et al. (1998). Results from 3 winter seasons compared in depth (DJF 1988/89, 1989/90, and 1990/91) indicate that low-frequency patterns, most notably the PNA, are embedded as leading spatial modes in five-day averaged atmospheric fields for North America (Derksen, 1998). When correlated with pentad SWE component loadings, the PNA-type patterns are negatively associated with central North American snow cover in a statistically stronger fashion (average correlation coefficient of 0.7) than the correlations produced in this study with monthly averaged data (average correlation coefficient of 0.5).

Spatial and Temporal Time Series Characteristics

The passive microwave derived imagery utilized in this study provide a unique dataset with associated strengths and weaknesses. All-weather imaging and rapid scene revisit ensure a continuous time series at a fine temporal resolution. In addition, the quantitative derivation of SWE provides data of both hydrological and climatological significance. No other remotely sensed data product can provide this level of information. Since this study has shown that SWE and SCA anomalies are not covariate, derivation of both these snow cover properties is significant.

The dependence of passive microwave algorithm performance on land cover, however, reduces the applicability of the data on a global scale, even though some algorithms have claimed global usage (for example, Grody and Basist, 1996). The dual channel algorithm used in this study is ground validated for the open Prairie environment only. The complex scattering which occurs within regions such as the boreal forest have necessitated specifc algorithm development (for example, Chang et al., 1997; Goita et al., 1997). The spatially constrained passive microwave study region can be considered a contributing factor to the generally weak correlations found in this study. Since analysis has shown that associations between specific atmospheric configurations and snow cover can vary regionally (Gutzler and Rosen, 1992), the limited ground validated region used in this study hampers the identification of associations simply due to the scope of the data.

In addition to the spatial limitation, passive microwave brightness temperatures in the EASE-Grid projection (required for studies of terrestrial snow cover) are readily available only since 1987. When Scanning Multichannel Microwave Radiometer (SMMR) data, which extend from 1978 to 1987, are released in the EASE-Grid format, the passive microwave time series will approach a more rigorous length. With sensors such as the Advanced Microwave Scanning Radiometer (AMSR) being prepared for imminent deployment, passive microwave data acquisition should continue uninterrupted. The ability to construct a thirty year normal from passive microwave data will therefore become reality. Questions must be answered, however, with respect to creating a full passive microwave time series. Can SMMR, SSM/I, and AMSR imagery be joined seamlessly to create a continuous data record? Do retrieval algorithms need to be adjusted given that each sensor provides slightly different measurement channels? If these, and related issues can be satisfactorily addressed, the characteristics of passive microwave imagery allow for analysis of a synoptically sensitive, temporally consistent dataset.

CONCLUSIONS

A rotated PCA has shown that winter season SWE distribution in central North America is subject to a high degree of interannual variability. While the first component adequately summarizes the variance in snow cover for three continuous seasons (1989/90 to 1991/92), unique components capture the variance for all other seasons. When the component loading patterns are related to total Prairie SWE and SCA standardized anomalies, no clear trend in snow cover is evident. Seasons with anomalously extensive snow cover are interspersed with deficit snow cover seasons.

A notable feature in the standardized anomaly time series is the frequency at which coincident SWE and SCA anomalies are of the opposed sign (21%). The magnitude of snow cover as expressed by SWE is not necessarily covariate to snow extent as expressed by SCA. Both of these variables, therefore, need to be considered within climatological studies.

When the pentad anomaly information and SWE component loading patterns were degraded to monthly averages and correlated to archived atmospheric teleconnection indices, associations were typically weak. The strongest associations are the negative correlations between the EP and PNA patterns and SWE and SCA anomalies at no time lag, and with the atmosphere leading by one month. The positive phase of these patterns are associated with deficit central North American snow cover, while the negative phase is linked to extensive snow cover.

This study produces no evidence to support snow cover as a forcing variable on atmospheric circulation. When the snow cover diagnostics (anomalies and component loadings) lead the atmospheric teleconnection indices by one month, correlation results are markedly lower than the opposed case. This confirms the results of other studies (for example, Foster et al., 1983; Dewey, 1987) which also found no basis for snow cover as a leading variable.

Total Prairie SWE and SCA are poorly autocorrelated over time, indicating a low temporal persistence to anomaly phase and magnitude. Given this rapidly changing state of snow cover, isolating cause and effect associations at a coarse monthly time scale is not a physically logical endeavour, even though this coarse resolution, long time series approach has been favoured (i.e. Karl et al., 1993; Leathers and Robinson, 1993; Serreze et al., 1998).

Atmospheric teleconnection indices provide a simple atmospheric diagnostic in the form of a standardized time series. As these teleconnections represent the preferred low-frequency atmospheric configurations, there is great predictive potential in their linkage to variability in terrestrial snow cover. The dynamic nature of rapidly evolving snow cover, however, limits the strength of associations which can be isolated between these variables. This study has shown that simple atmospheric diagnostics are inadequate for linking snow cover and atmospheric circulation alone. Since teleconnection patterns are evident within synoptically sensitive gridded atmospheric fields, the potential exists to improve our predictive understanding of associations between snow cover and the atmosphere, utilizing teleconnection indices as a resource.

ACKNOWLEDGMENTS

This work was supported by funding through the Canadian Atmospheric Environment Service Science Subvention and a CRYSYS contract (E. LeDrew), and the Natural Science and Engineering Research Council (operating grant - E. LeDrew, scholarship - C. Derksen). The SSM/I EASE-Grid data were obtained from the EOSDIS National Snow and Ice Data Center Distributed Active Archive Center (NSIDC DAAC), University of Colorado at Boulder. Thanks are extended to Joe Piwowar and Ryan Draper for assistance with data preparation.

References

Barnston, A., and R. Livezey. 1987. Classification, seasonality and persistence of low-frequency atmospheric circulation patterns. Monthly Weather Review. 115: 1083-1126.

Cayan, D. 1996. Interannual climate variability and snowpack in the Western United States. Journal of Climate. 9(5): 928-948.

Chang, A., J. Foster, D. Hall, B. Goodison, A. Walker, J. Metcalfe, and A. Harby. 1997. Snow parameters derived from microwave measurements during the BOREAS winter field campaign. Journal of Geophysical Research. 102(D24): 29 663-29 671.

Clark, M., M. Serreze, and D. Robinson. 1999. Atmospheric controls on Eurasian snow extent. International Journal of Climatology. 19: 27-40.

Cohen, J., and D. Rind. 1991. The effect of snow cover on the climate. Journal of Climate. 4(7): 689-706.

Derksen, C., E. LeDrew, and B. Goodison. 1998. SSM/I derived snow water equivalent data: the potential for investigating linkages between snow cover and atmospheric circulation. Atmosphere-Ocean. 36(2): 95-117.

Derksen, C. 1998. Associations between passive-microwave derived Prairie snow cover and atmospheric circulation. Waterloo Laboratory for Earth Observations Technical Report 99-002, University of Waterloo, Waterloo, Ontario, Canada.

Derksen, C., and E. LeDrew. 1999. The influence of sensor overpass time on passive microwave derived snow water equivalent measurements. CD-ROM Proceedings, International Geoscience and Remote Sensing Symposium, Hamburg, Germany, July, 1999.

Foster, J., M. Owe, and A. Rango. 1983. Snow cover and temperature relationships in North America and Eurasia. Journal of Climate and Applied Meteorology. 22: 460-469.

Foster, J. A. Chang, D. Hall. 1997. Comparison of snow mass estimates from a prototype passive microwave snow algorithm, a revised algorithm and a snow depth climatology. Remote Sensing of Environment. 62: 132-142.

Goita, K., A. Walker, B. Goodison, and A. Chang. 1997. Estimation of snow water equivalent in the boreal forest using passive microwave data. In CD-ROM Proceedings, Geomatics in the Era of Radarsat, Ottawa, Ontario, May, 1997.

Goodison, B., I. Rubinstein, F. Thirkettle, and E. Langham. 1986. Determination of snow water equivalent on the Canadian Prairies using microwave radiometry. Modelling Snowmelt Induced Processes, Proceedings of the Budapest Symposium, July 1986. 163-173.

Goodison, B., and A. Walker. 1994. Canadian development and use of snow cover information from passive microwave satellite data. In Choudhury, B., Y. Kerr, E.Njoku, and P. Pampaloni (eds.). Passive Microwave Remote Sensing of Land-Atmosphere Interactions. VSP BV, Utrecht, Netherlands, 245-262.

Grody, N., and A. Basist. 1996. Global identification of snowcover using SSM/I measurements. IEEE Transactions on Geosciences and Remote Sensing. 34(1):237-249.

Gutzler, D., and R. Rosen. 1992. Interannual variability of wintertime snow cover across the Northern Hemisphere. Journal of Climate 5:1441-1447.

Karl, T., P. Groisman, R. Knight, and R. Heim. 1993. Recent variations of snow cover and snowfall in North America and their relation to precipitation and temperature variations. Journal of Climate. 6:1327-1344.

Lanzante, J. 1984. A rotated eigenanalysis of the correlation between 700 mb heights and sea surface temperatures in the Pacific and Atlantic. Monthly Weather Review. 102: 2270-2280.

Leathers, D., and D. Robinson. 1993. The association between extremes in North American snow cover extent and United States temperatures. Journal of Climate 6(7): 1345-1355.

Overland, J., and R. Preisendorfer. 1982. A significance test for principal components applied to a cyclone climatology. Monthly Weather Review. 110(1): 1-4.
Richman, M. 1986. Rotation of principal components. Journal of Climatology. 6: 293-335.
Serreze, M., M. Clark, D. McGinnis, and D. Robinson. 1998. Characteristics of snowfall over the eastern half of the United States and relationships with principal modes of low-frequency atmospheric variability. Journal of Climate. 11: 234-250.
Tait, A. 1998. Estimation of snow water equivalent using passive microwave radiation data. Remote Sensing of Environment. 64: 286-291.
Walker, A. and B. Goodison. 1993. Discrimination of a wet snow cover using passive microwave satellite data. Annals of Glaciology. 17: 307-311.
Wallace, J. and D. Gutzler. 1981. Teleconnections in the potential height field during the Northern Hemisphere winter. Monthly Weather Review. 109: 784-812.
Walsh, J., and C. Johnson. 1979. Interannual atmospheric variability and associated fluctuations in Arctic sea ice extent. Journal of Geophysical Research. 84: 6915-6928.
Walsh, J., D. Tucek, and M. Peterson. 1982. Seasonal snow cover and short-term climatic fluctuations over the United States. Monthly Weather Review. 110: 1474-1485.
Walsh, J. 1984. Snow cover and atmospheric variability. American Scientist. 72:50-57.